This is an open access article published under an ACS AuthorChoice License, which permits copying and redistribution of the article or any adaptations for non-commercial purposes.

ACS Catalysis

Research Article

pubs.acs.org/acscatalysis

Fe-Porphyrin-Based Metal–Organic Framework Films as High-Surface Concentration, Heterogeneous Catalysts for Electrochemical Reduction of CO_2

Idan Hod,[†,∥] Matthew D. Sampson,[‡] Pravas Deria,[†] Clifford P. Kubiak,*[,‡] Omar K. Farha,*[,†,∥,§] and Joseph T. Hupp*[,†,∥,⊥]

[†]Department of Chemistry, Northwestern University, 2145 Sheridan Road, Evanston, Illinois 60208, United States

[‡]Department of Chemistry and Biochemistry, University of California at San Diego, 9500 Gilman Drive, La Jolla, California 92093-0358, United States

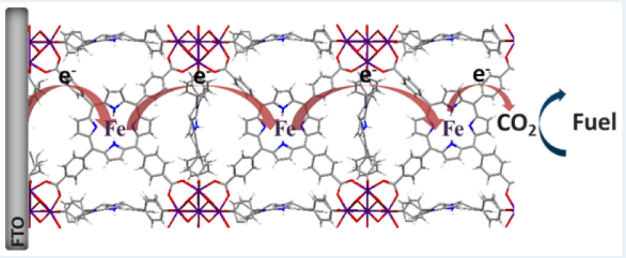
[§]Department of Chemistry, Faculty of Science, King Abdulaziz University, Jeddah, Saudi Arabia

[∥]Argonne-Northwestern Solar Energy Research (ANSER) Center, Northwestern University, 2145 Sheridan Road, Evanston, Illinois 60208, United States

[⊥]Argonne National Laboratory, 9700 South Cass Avenue, Argonne, Illinois 60439, United States

Supporting Information

ABSTRACT: Realization of heterogeneous electrochemical CO_2-to-fuel conversion via molecular catalysis under high-flux conditions requires the assembly of large quantities of reactant-accessible catalysts on conductive surfaces. As a proof of principle, we demonstrate that electrophoretic deposition of thin films of an appropriately chosen metal–organic framework (MOF) material is an effective method for immobilizing the needed quantity of catalyst. For electrocatalytic CO_2 reduction, we used a material that contains functionalized Fe-porphyrins as catalytically competent, redox-conductive linkers. The approach yields a high effective surface coverage of electrochemically addressable catalytic sites (~10^{15} sites/cm^2). The chemical products of the reduction, obtained with ~100% Faradaic efficiency, are mixtures of CO and H_2. These results validate the strategy of using MOF chemistry to obtain porous, electrode-immobilized, networks of molecular catalysts having competency for energy-relevant electrochemical reactions.



KEYWORDS: *CO_2 reduction, electrocatalysis, metal organic frameworks, Fe-porphyrin, solar fuel, redox conductivity*

INTRODUCTION

The reduction of carbon dioxide to useful chemical fuels holds great promise for slowing the growth of humanity's enormous carbon footprint. When reduction reactions are driven by a renewable energy source, such as sunlight, they can provide a route to carbon-neutral energy.[1] Nevertheless, simple CO_2 reduction is an energetically and kinetically challenging process. The one-electron reduction of CO_2 to $CO_2^{\bullet-}$ has a very high thermodynamic threshold, approximately −2 V versus the normal hydrogen electrode (NHE).[2−4] More favorable in terms of electrochemical thermodynamics (i.e., formal potentials for half-reactions) are proton-coupled, multielectron reduction reactions. These lead to a variety of products such as carbon monoxide (CO) and formic acid (two electrons each), formaldehyde (four electrons), methanol (six electrons), and methane (eight electrons).[2] However, slow kinetics for these complex processes demands the introduction of efficient catalysts to decrease the overpotential needed to drive them. Extensive research effort has been invested in developing molecular catalysts for photochemical and/or electrochemical reduction of CO_2. Among the catalysts are a variety of redox-active metal complexes, including complexes of Fe,[5−10] Re,[1,11−15] Ni,[16−19] Co,[20,21] Mn,[22−24] and Ru.[25,26]

Systems based on molecular catalysts in homogeneous solutions are mainly attractive for two reasons: (1) reaction intermediates are comparatively easy to spectroscopically characterize, thereby facilitating elucidation of the mechanistic details of the catalytic reaction, and (2) modulation of the catalyst structure to suit the appropriate catalytic process can be achieved in a straightforward manner through synthetic means. However, homogeneous catalysts are only electro-activated at or near the surface of a conductive electrode. Heterogeneous electrocatalysis offers the possibility of overcoming this and other drawbacks often associated with homogeneous electrocatalysis. Thus, the use of catalysts in heterogeneous form has the potential to eliminate deactivation processes such as

Received: August 12, 2015
Revised: September 17, 2015
Published: September 18, 2015

Downloaded via LBRY FOR NATURAL SCIENCES RAS on August 23, 2018 at 10:31:09 (UTC).
See https://pubs.acs.org/sharingguidelines for options on how to legitimately share published articles.

© 2015 American Chemical Society

DOI: 10.1021/acscatal.5b01767
ACS Catal. 2015, 5, 6302−6309

dimerization or aggregation of the highly active catalyst species[27] (thereby increasing the lifetime of the catalytic system), provide better control of the chemical surroundings of the catalyst's active site for improved performance,[28] and permit the use of solvents that otherwise could not be employed because of the catalyst's poor solubility.[29] Heterogenization additionally eliminates the possible problem, in a complete catalytic cell, of keeping the reduction catalyst away from the electrode where the corresponding oxidation half-reaction (for example, water to O_2) is occurring. (Contact with the anode holds the possibility of interference of the catalyst with the oxidation reaction, as well as oxidative degradation of the catalyst.)

Several examples of heterogeneous electrocatalytic CO_2 reduction systems based, on immobilization of molecular catalysts on electrode surfaces, are known. The means of immobilization include covalent bonding of molecular monolayers,[30,31] noncovalent molecular attachment,[32,33] and surface polymerization of permeable, molecular-catalyst multilayers.[34−38] In part due to the fact that planar electrode geometries are most often used, the amount (i.e., areal concentration or surface coverage) of heterogenized molecular catalysts has thus far been limited to $\sim 10^{-12}$ mol/cm^2 (submonolayers) to $\sim 10^{-8}$ mol/cm^2 (multilayers, albeit of limited molecular-scale porosity or permeability).[30−34,39]

In an EC′ type of catalytic mechanism,[41] the first step is electron transfer (E) from the electrode to the catalyst, reducing it to its active form, which in turn chemically reacts (C′) with a substrate to form the reaction products. The magnitude of the steady state current density (and thus overall catalytic rate) for a given EC′ system (whether homogeneous or heterogeneous) is governed by both the rate of the reaction of the substrate with the individual molecular catalyst and the active-catalyst concentration.[3,41] A key difference between catalytic heterogeneous (i.e., electrode-immobilized) and homogeneous (i.e., solution-dissolved) molecular systems is that the overall reaction kinetics for heterogeneous systems are not limited by the rate of diffusion of the catalyst toward the electrode, nor are overall rates in the heterogeneous case limited by catalyst solubility. Thus, for heterogeneous systems, enhancement of either the molecular-scale reaction rate or the active-catalyst areal concentration[42] may, in principle, lead to higher overall rates (greater catalytic current densities) at a given applied potential.[41] It is clear, then, that a significant leap in catalytic performance may be anticipated if one can drastically increase the amount of stable, surface-bound catalyst.

With this notion in mind, we have realized the potential in employing metal−organic framework (MOF) thin films[43] as a high-surface area platform to substantially boost the areal concentration of a molecular CO_2 reduction catalyst. In contrast to a densely packed polymerized film, a MOF creates an ordered, porous heterogeneous network, which allows for free permeation of electrolyte counterions and dissolved CO_2 into the interior of the film.[44−47] To realize our hypothesis, first the MOF should possess the ability to transport electrons from the current collector toward the electrocatalyst to drive the reaction. Several recent studies have established that charge transport can occur within MOF films, following the mechanism of either linker-to-linker[48−51] or shuttle-to-shuttle[52] electron/hole redox hopping. Consequently, a MOF having a redox-active molecular catalyst as a linker could constitute a candidate heterogeneous electrocatalytic system (an especially germane example is the recent work of Ahrenholtz et al.[48] involving the electrocatalytic degradation of carbon tetrachloride by the metallo-porphyrinic MOF, cobalt-PIZA-1[53]). We note that earlier important work reported on high current densities for CO_2 reduction using molecular-catalyst-impregnated porous gas-diffusion carbon electrodes.[54] However, this system lacked the structural ordering of a well-defined, crystalline MOF film. In addition, the catalyst was unevenly loaded into the porous carbon matrix. As a result, accurate elemental and physical characterization (for instance, degree of film porosity or the position/attachment mode of immobilized catalyst) of gas-diffusion carbon electrodes is much more challenging compared to that of a MOF system. Moreover, the immobilization of the molecular catalyst using a MOF offers the opportunity to avoid aggregation and deactivation processes because of the physical separation between each of the catalyst molecules, achieved by their covalent attachment to the framework nodes.

Here, we have used the well-known Fe-porphyrin CO_2 reduction catalyst as a test system, incorporating the porphyrin into a MOF as both a structural and functional element, with the MOF being deployed in a thin-film electrode-immobilized form. Iron-porphyrin complexes have been extensively studied for electrocatalytic reduction of CO_2 to CO by Savéant and coworkers.[6−9] When those samples are dissolved in nominally nonaqueous solutions under an inert atmosphere, three distinct reduction waves are observed in cyclic voltammetry (CV) measurements, corresponding to the Fe(III/II), Fe(II/I), and Fe(I/0) couples. Previous studies have shown that in CO_2-saturated solutions, the Fe(I/0) wave becomes enhanced and irreversible, typical of a catalytic process, indicating that the Fe(0)-porphyrin species is the active catalyst for CO_2 reduction. As shown in Figure 1, similar behavior was readily observed in our laboratories.

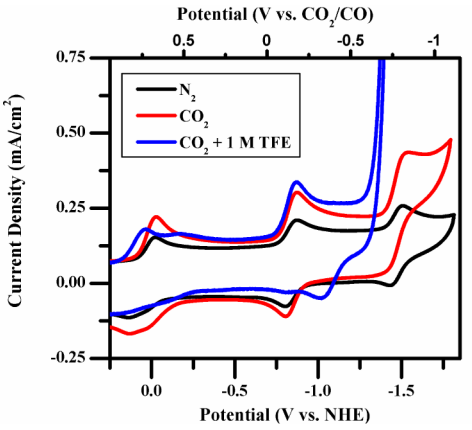


Figure 1. Cyclic voltammograms of homogeneous Fe-TPP (1 mM) in dimethylformamide (scan rate of 0.1 V/s). Comparison between N_2 (black) and CO_2 atmosphere, with no added proton source (red) and with 1 M added trifluoroethanol (TFE) proton source (blue), showing the catalytic current rise with added TFE.

Herein, we demonstrate the use of a thin film of Fe-porphyrin-based MOF-525[40,55] [Fe_MOF-525 (Figure 2)] as a platform for anchoring a substantial quantity of an electroactive molecular catalyst on a conductive electrode for electrochemical reduction of CO_2. We chose MOF-525 as the catalyst immobilizer, in part because of its good molecular-scale porosity, but also because of its excellent chemical stability, an important requirement for a robust electrocatalytic assembly.

DOI: 10.1021/acscatal.5b01767
ACS Catal. 2015, 5, 6302−6309

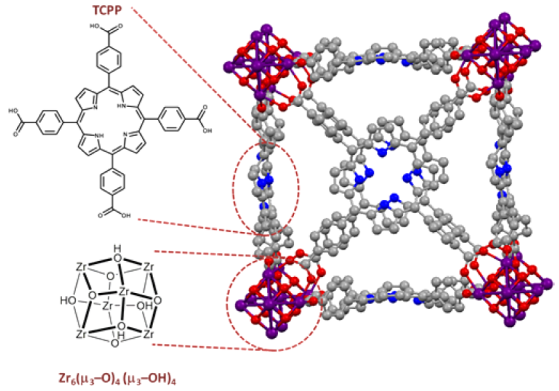


Figure 2. Illustration of a portion of the crystal structure of MOF-525 in porphyrin free-base form,[40] including the chemical structure of the TCPP linker and the Zr_6-based node.

(Superior chemical stability is a consequence of the use of hexa-zirconium(IV) nodes, together with carboxylate-based linker binding.[56−59]) Reductive potential step analysis of the Fe_MOF-525 film revealed an effective catalyst surface concentration roughly 3 orders of magnitude higher than the estimated catalyst monolayer coverage and close to 1 order of magnitude higher than any previously reported loading for a heterogenized molecular CO_2 reduction catalyst (albeit comparable to the surface concentration reported by Ahrenholtz et al. for a MOF-based catalyst for electrochemical reduction of carbon tetrachloride[48]). CV measurements, under both N_2 and CO_2, confirmed that the Fe-porphyrin linker of Fe_MOF-525 is responsible for electrocatalysis, with a catalytic wave evident at the potential of the Fe(I/0) couple. In addition, bulk electrolysis experiments showed sizable current densities, with mixtures of CO and H_2 as products.

EXPERIMENTAL SECTION

Instrumentation. Thin-film XRD patterns were measured on a Rigaku ATX-G thin-film diffraction workstation. Scanning electron microscopy (SEM) images and energy dispersive X-ray spectroscopy (EDS) data were collected on a Hitachi SU8030 instrument.

All cyclic voltammetry (CV) experiments were performed on either a Solarton Analytical Modulab Potentiostat or a Gamry Epsilon Potentiostat. A three-electrode electrochemical setup was used, with a platinum mesh counter electrode, Ag/AgCl/KCl (saturated) electrode as a reference electrode, and the Fe_MOF-525 thin-film/FTO working electrode (active area of 1 cm^2). For all measured CVs, the scan rate was 100 mV/s.

Electrophoretic Deposition of MOF Thin Films.[49,60] Ten milligrams of MOF powder was suspended in a 20 mL toluene solution and sonicated for 30 s. Two identical fluorine-doped tin oxide (FTO) glass substrates (15 Ω/sq, Hartford Glass) were dipped in the deposition solution (1 cm separation distance), and a constant DC voltage of 130 V was applied using an Agilent E3 612A DC power supply. The duration of deposition was 3 h. **Caution:** *Electrical sparking due to accidental contact of electrodes and/or their leads can result in ignition of toluene. The electrophoretic deposition procedure should be done in a fume hood, clear of flammables.*

Postmetalation of the MOF-525 Thin Films. Ten milligrams of iron chloride was dissolved in 10 mL of dimethylformamide (DMF) in an eight-dram vial. The MOF-525 thin film was placed into the vial, and the closed vial was placed into an oven at 80 °C for 24 h. The obtained thin film was removed from the solution, washed several times with DMF and acetone, and dried under vacuum.

Bulk Electrolysis Measurements. Controlled potential electrolysis (CPE) experiments (at approximately −1.3 V vs NHE) were conducted in a 60 mL Gamry five-neck cell with a three-electrode setup: platinum counter electrode in a fritted glass compartment, a leakless Ag/AgCl reference electrode (eDAQ), and either the Fe_MOF-525 thin-film/FTO working electrode (active area of 1 cm^2) or a glassy carbon rod working electrode (surface area of 7.4 cm^2). A BASi Epsilon potentiostat was used to apply constant potential and record current. These CPE experiments were conducted in 30 mL of the total electrolyte solution (1 M $TBAPF_6$ in DMF; for our purposes, the Fe-TPP molecular catalyst proved to be insufficiently soluble in acetonitrile). Electrochemical solutions were first bubbled with N_2 for 5 min and then bubbled with CO_2 for 15 min before the experiments. Solutions were constantly stirred (at a consistent rate for all experiments) throughout each CPE experiment. Gas analysis for CPE experiments were performed using 1 mL sample injections on a Hewlett-Packard 7890A Series gas chromatograph with two molsieve columns [30 m × 0.53 mm (inside diameter) × 25 μm film]. The 1 mL injection was split between two columns, one with N_2 as the carrier gas and one with He as the carrier gas, to quantify both H_2 and CO simultaneously in each run. Gas chromatography calibration curves were made by sampling known volumes of CO and H_2 gas. CPE experiments for Fe_MOF-525 films were conducted in a similar manner (see the Supporting Information for more details).

RESULTS AND DISCUSSION

MOF-Film Formation and Characterization. Microcrystalline MOF-525 particles were synthesized via a solvothermal route according to a previously reported procedure[55] (see the Supporting Information). The MOF contains TCPP [meso-tetra(4-carboxyphenyl)porphyrin] linkers and hexa-zirconium nodes, assembled to form interconnected boxes [cubes (see Figure 2)]. Thin films of MOF-525 on FTO were then obtained from a toluene suspension of microcrystalline MOF powder via electrophoretic deposition (EPD).[49] The films were infiltrated with an $FeCl_3$ solution, and the free-base porphyrin linkers reacted to give the desired Fe_MOF-525 films (see Figure S1). SEM images (Figure 3a) show that EPD-formed films consist of cubic particles 300−500 nm in size. PXRD measurements (Figure 3b) confirm that the films are composed of MOF-525. Energy dispersive X-ray

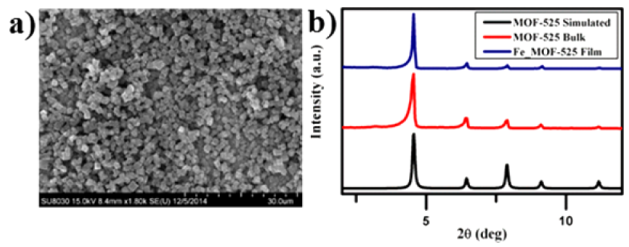


Figure 3. (a) Scanning electron microscopy image of a Fe_MOF-525 thin film, exhibiting the typical cubic morphology of MOF-525. (b) PXRD comparison between simulated, bulk powder and thin film diffraction patterns. Upon film fabrication, the Fe_MOF-525 particles retain their crystal structure.

DOI: 10.1021/acscatal.5b01767
ACS Catal. 2015, 5, 6302−6309

spectroscopy (EDS) yielded a Zr_6:Fe ratio of 1:2.8, which is equivalent to 93% metalation (see Figure S1b). EDS mapping measured across a single Fe_MOF-525 crystallite revealed a uniform distribution of Fe (Figure S2).

To assess the electroactivity of the prepared Fe_MOF-525 films, CV measurements were conducted in a 1 M $TBAPF_6$ acetonitrile solution under a N_2 atmosphere, with a standard three-electrode configuration containing the Fe_MOF-525 film, a Ag/AgCl (saturated KCl) electrode, and a Pt mesh as the working, reference, and counter electrodes, respectively (Figure 4a). When the electrochemical potential is scanned in the reductive direction, three distinct redox waves were observed, which can be attributed to Fe(III/II) (E_f = −0.32 V vs NHE), Fe(II/I) (E_f = −0.87 V vs NHE), and Fe(I/0) (E_f ∼ −1.4 V vs NHE).[61,62] These electrochemical features demonstrate the ability of the Fe_MOF-525 film to transfer charge by redox hopping between neighboring Fe-TCPP sites.

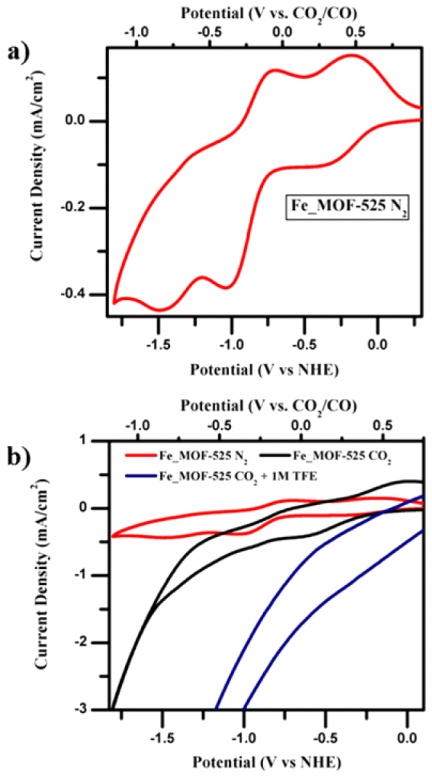


Figure 4. Cyclic voltammograms of Fe_MOF-525 films in a 1 M $TBAPF_6$ acetonitrile solution: (a) under a N_2 atmosphere, demonstrating the redox hopping ability of the Fe_MOF-525 film; (b) comparing behavior in N_2- vs CO_2-saturated solutions, with and without addition of a 1 M trifluoroethanol (TFE) proton source, showing electrocatalytic CO_2 reduction behavior.

The amount of electroactive catalyst was measured by chrono-amperommetry. When the potential was stepped from 0.2 to −0.5 V versus NHE [reducing the Fe(III) to Fe(II)], the current decay over time was recorded (Figure S3). From the charge passed, an electrocatalyst surface concentration of 6.2 × 10^{-8} mol/cm^2 was obtained. Visible-region spectroelectrochemistry measurements show that 77% of the electrophoretically deposited porphyrin sites are electrochemically addressable in the region of the Fe(III/II) couple (Figure S4). In contrast, estimation of the surface concentration of TCPP molecules on a flat electrode (TCPP area of 2.5 nm^2), assuming full packing, gives only 7 × 10^{-11} mol/cm^2. In other words, the use of Fe_MOF-525 on a FTO electrode increased the amount of active catalyst by ∼3 orders of magnitude, as compared to a monolayer of catalyst immobilized on the same flat electrode. To the best of our knowledge, no previously heterogenized molecular CO_2 reduction catalysts have been installed at surface concentrations (areal concentrations) higher than 1 × 10^{-8} mol/cm^2, emphasizing the advantage of using the MOF as a strategy to boost the catalyst quantity and catalytic performance.

MOF-Film-Based Electrocatalysis. We assessed the MOF film's performance as an electrocatalyst for CO_2 reduction. As shown in Figure 4b and Figure S5, compared to a N_2 atmosphere, upon saturation of a 1 M $TBAPF_6$ acetonitrile electrolyte solution with CO_2, the Fe(I/0) redox wave shows catalytic behavior and exhibits an increase in current density, suggesting CO_2 reduction at this potential.

To confirm that the current increase is due to catalytic CO_2 reduction, we subjected a Fe_MOF-525-containing cell to controlled potential electrolysis (CPE) at a constant working electrode potential of −1.3 V versus NHE. Figure 5 summarizes the CPE behavior over time, showing (a) current density, (b and c) turnover numbers (TONs) for CO and H_2 formation, and (d) Faradaic efficiency of the Fe_MOF-525 films in an acetonitrile solution as compared to a bare FTO electrode. The Fe_MOF-525 system reached current densities of up to 2.3 mA/cm^2 after electrolysis for 30 min. The remainder of the experiment showed a slow decline in current density attributed to catalyst degradation (Figure 3a). Gas chromatographic analysis after CPE for >4 h indicated that the Fe_MOF-525 generated two products: CO and H_2 (15.3 and 14.9 μmol/cm^2 of CO and H_2, respectively). Taking into account the amount of electroactive catalyst in the film (6.2 × 10^{-8} mol/cm^2), these values correspond to a CO TON of 272 and an average turnover frequency (TOF) of 64 h^{-1} (Figure 5b).[63]

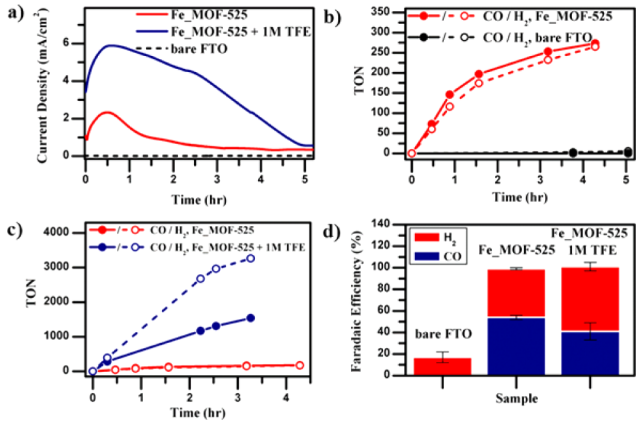


Figure 5. Controlled potential electrolysis of Fe_MOF-525 in 1 M $TBAPF_6$ acetonitrile solutions. (a) Current density vs time for Fe_MOF-525 without added TFE (red), Fe_MOF-525 with added TFE (blue), and a bare FTO blank (black). (b) TON vs time for Fe_MOF-525 without added TFE (red) and a bare FTO blank (black). (c) TON vs time for Fe_MOF-525 without added TFE (red) and Fe_MOF-525 with added TFE (blue). (d) Faradaic efficiency over approximately 4 h of electrolysis.

Even without an intentionally added proton source, the amount of H_2 evolved during the CPE experiments is nontrivial. Dihydrogen presumably derives from electro-

DOI: 10.1021/acscatal.5b01767
ACS Catal. 2015, 5, 6302−6309

chemical reduction of residual water in the organic solvent (acetonitrile),[62] or from abstracting a proton from the $TBAPF_6$ electrolyte via Hofmann-type degradation.[64] A second role for trace water may be to consume the dianionic oxygen atom lost upon conversion of CO_2 to CO. The produced mixtures of CO and H_2 (Faradaic efficiencies of 54 ± 2 and 45 ± 1% for CO and H_2 formation, respectively) could be directly converted to useful hydrocarbons by the Fischer−Tropsch (FT) process. (The optimal CO:H_2 ratio for FT reactions varies depending on the type of catalyst, the operating temperature, and the hydrocarbon products desired.)[65] As expected, the bare FTO electrode showed no catalytic activity for reduction of CO_2 to CO and produced only trace amounts of H_2 (Figure 5b).

In electrocatalysis studies with homogeneous Fe-TPP in (nominally) nonhydroxylic solvent, it has been shown that the addition of weak Brönsted acids, such as 2,2,2-trifluoroethanol (TFE), elicits a significant improvement in both catalytic current densities and system stability.[8,66] The improvements are a result of the ready protonation of the Fe−CO_2 adduct, which facilitates C−O bond cleavage and release of the CO product.[5,67] The added acid also provides a way of stabilizing the released oxygen anion (as water).[68] As shown in Figure 5a, upon addition of 1 M TFE, the Fe_MOF-525 system exhibited significantly increased current densities, up to 5.9 mA/cm^2, as well as increased catalyst stability. CPE experiments with added TFE, at E = −1.3 V versus NHE, resulted in a 7-fold increase in CO production, with the CO TON reaching 1520 (average TOF of 0.13 s^{-1}) after electrolysis for 3.2 h (Figure 5c). As shown in Figure 5d, Faradaic efficiencies are 41 ± 8 and 60 ± 4% for CO and H_2 formation, respectively, meaning that the total Faradaic efficiency (CO + H_2) of the Fe_MOF-525 system is ∼100%, both with and without TFE.[69] At −1.3 V versus NHE, CV experiments (Figure 4b and Figure S5) return a catalytic current similar to the average current in the CPE experiment, i.e., 4 mA/cm^2. Notable in the CV measurements is the presence of significant catalytic current well positive of the formal potential for the film-based Fe(I/0) couple, approximately −1.4 V.

Comparisons to Homogeneous Catalysis. Figure 1 and Figure S6 show electrochemical CV responses for a 1 mM solution of Fe-TPP in 30 mL of CO_2-saturated DMF (230 mM CO_2),[70] with and without 1 M TFE (thus, the total number of moles of catalyst is 3 × 10^{-5}). Figure 6 and Figure S7a show the behavior of the homogeneous catalyst during constant potential electrolysis (−1.3 V vs NHE). Over a 6 h period, in 30 mL of stirred CO_2-saturated acetonitrile containing 1 M TFE, the 1 mM catalyst solution yields a nearly constant catalytic current of ∼12 mA/cm^2.

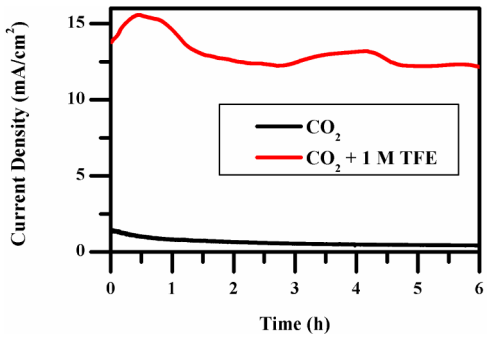


Figure 6. Controlled potential electrolysis of homogeneous Fe-TPP in a 1 M $TBAPF_6$ DMF solution. Current density vs time for Fe-TPP without added TFE (black) and with added TFE (red).

From Figure 1 (homogeneous Fe-TPP), the catalytic current is strongly dependent on potential, much more strongly dependent than for the heterogenized MOF-based catalyst (Figure 4). The fact that catalytic current can be easily observed at potentials positive of Fe(I/0) implies that Fe(0)-TPP is strongly catalytic for CO_2 reduction, a point previously emphasized by Saveant and co-workers for this catalyst system.[6−8] Because only a tiny fraction of the dissolved homogeneous catalyst is present at any given time within the reaction zone of the electrode, it is comparatively uninformative to calculate TOF (or TON) values based on the total amount of catalyst in solution. Instead, we have used Saveant's foot-of-the-wave analysis.[70] From the analysis (see the Supporting Information for details), the second-order rate constant for Fe-TPP reduction of CO_2 to CO is 2400 M^{-1} s^{-1}. The TOF at E = −1.3 V versus NHE is 2.1 s^{-1}. These values, while larger than for many molecular electrocatalysts, are consistent with Saveant's observations.[70]

A plot of E versus log(TOF) yields a slope of approximately −53 mV/decade-TOF (see Figure S8a,b), close to the value of −59 mV/decade-TOF expected if the Nernst equation, rather than the kinetics of interfacial electron transfer, describes the fraction of metalloporphyrin present at the solution−electrode interface in the catalytically active Fe(0) form. By plot extrapolation, the TOF at E = −1.25 V is 0.3 s^{-1} while at E = −1.2 V it is 0.043 s^{-1}.

With respect to the results obtained at −1.3 V versus NHE, the homogeneous catalyst (Fe-TPP) displays a TOF that is 16 times higher than that of the heterogeneous version (Fe_MOF-525). This observation raises intriguing questions. First, why are the catalytic activities of the immobilized catalyst and the homogeneous catalysts so different? Second, how can the TOF for the immobilized catalyst be so small relative to that of the homogeneous catalyst yet support catalytic currents that are within a factor of 2 or 3 of that of the homogeneous catalyst? Third, why is the catalytic current with Fe_MOF-525 so much less dependent on the applied potential than is the catalytic current produced with the homogeneous species?

Catalyst heterogenization via porous MOF formation occurs beyond the perimeter of the catalyst, at carboxylate linkages on pendant phenyl groups. As such, it seems unlikely that the intrinsic activity of the catalyst—as influenced, for example, by substituent or environmental electronic effects—is affected significantly by MOF formation. If electronic attenuation is unimportant, then other factors must be limiting the TOF. Figure 4a offers a hint: the voltammetric wave for the Fe(I/0) couple is distorted in a way that suggests slow diffusion, presumably of either electrons hopping from site to site (iron to iron) or ions moving in charge-compensating fashion (the porphyrin sites themselves, of course, are spatially fixed).[71]

The notion of rate-limiting charge diffusion is supported by variable scan rate CV studies that show that the voltammetric peak current increases as the square root of the voltammetric scan rate, rather than linearly [as expected if diffusive limitations are unimportant (see Figure S9)]. Chronoamperometry measurements (see Figure S10) permit the charge-diffusion coefficient, D, to be quantified and yield a value of 5 × 10^{-13} cm^2 s^{-1}. While the value is tiny in comparison to diffusion coefficients for small molecules in conventional solutions, it is not grossly out of line with the few values reported for MOF-based charge transport.[48] It is important to recognize as well

DOI: 10.1021/acscatal.5b01767
ACS Catal. 2015, 5, 6302−6309

that the relevant transport distances are comparatively small, as the thickness of the MOF-525 film is only on the order of several hundreds of nanometers; thus, complete charge diffusion and concomitant film reduction from Fe(I) to Fe(0) require on the order of only a few to several seconds. Nevertheless, these times are approximately an order of magnitude greater than the time required for turnover of a single Fe-TPP catalyst outside the MOF environment (i.e., 0.5 s at −1.3 V vs NHE). We conclude, therefore, that at $E = -1.3$ V versus NHE the rate of catalytic reduction of CO_2 by the MOF film is largely limited by the rate of charge diffusion.

The ability of the MOF to provide catalytic currents that are within a factor of 2 or 3 of those obtained with the homogeneous catalyst, despite the 16-fold difference in effective TOF values, is a consequence of the MOF-based concentration and immobilization of Fe-TPP catalysts at or near the electrode surface. Thus, 1 cm^2 of densely packed (but porous) MOF film places 0.6 μmol of electrochemically addressable catalyst within 1 μm or less of the electrode surface. In contrast, the millimolar homogeneous solution of Fe-TPP places 1 nmol/cm^2 of catalyst, 600-fold less, within a μm or less of the electrode (albeit, with the likelihood of fresh catalyst diffusing in as the initial catalyst undergoes reaction).

Furthermore, a comparison between log(TOF) as a function of overpotential for homogeneous Fe-TPP (extracted using foot-of-the-wave analysis) and heterogeneous Fe_MOF-525 (extracted using the obtained current density at each potential, assuming similar faradaic efficiencies for all potentials) is given in Figure S8c. As one can see, the comparatively weak dependence of the MOF-derived catalytic current on electrode potential implies that even as the potential is made less negative and the TOF for the homogeneous catalyst sharply drops, the heterogeneous process remains largely limited by diffusive charge transport rather than molecular-scale kinetics for catalytic conversion. Consequently, at slightly lower overpotentials, a cross-point between the TOF of both systems is obtained, at which the TOF values for the homogeneous catalyst become smaller than those of the heterogeneous version. Thus, the TOF value for the MOF-immobilized catalyst at $E = -1.25$ V is 0.12 s^{-1} (compared to 0.3 s^{-1} for the homogeneous catalyst), but at −1.2 V, TOF for the MOF-immobilized catalyst is 0.11 s^{-1} (compared to 0.043 s^{-1} for the homogeneous catalyst). Nevertheless, for the heterogenized catalyst to match or exceed the catalytic current density achieved by the homogeneous catalyst at $E = -1.3$ V versus NHE, it is clear that faster charge transport (charge diffusion) will be required. Understanding what limits redox-based charge transport through MOF materials is the focus of ongoing studies, as are investigations of methods for boosting rates of charge diffusion. While not explored here, we find that charge transport through Fe_MOF-525, as indicated by apparent diffusion coefficients, is ∼20 times faster when based on the Fe(III/II) couple than on the catalytically relevant Fe(I/0) couple. We will report elsewhere on the chemical basis for this large difference.

Finally, Figure 5a implies that after CPE for 5 h, the MOF-based catalyst has largely degraded. In contrast, on the basis of Figure 6, the homogeneous catalysis appears to degrade only slightly, if at all, over the course of CPE for 6 h. It is important to note, however, that the total amount of catalyst present in the homogeneous CPE experiment is ∼50-fold greater than in the heterogeneous experiment. Assuming that degradation is associated with catalytic cycling and recognizing that catalyst molecules in homogeneous solution both freely diffuse and are subjected to controlled convection (solution stirring), very few homogeneous catalyst molecules will experience the number of catalytic turnovers experienced by MOF-immobilized catalyst molecules.

CONCLUSIONS

Electrophoretic deposition of crystallites of appropriately chosen MOFs is an effective means of heterogenizing and surface-concentrating catalysts for the electrochemical reduction of CO_2. Using Fe_MOF-525, we find that the well-known CO_2 reduction catalyst Fe-TPP can be installed on electrode surfaces at high areal concentrations equivalent to ∼900 monolayers of surface-adsorbed Fe-TPP, and almost an order of magnitude higher than the highest previous report on heterogenized molecular CO_2 reduction catalysts. Importantly, the well-defined nanoscale porosity of the MOF facilitates access of the solvent, reactant, and electrolyte to the surfeit of catalytic sites. The MOF's metalloporphyrinic linkers serve as both electrocatalysts and as redox-hopping-based conduits for the delivery of reducing equivalents to catalytic sites that are not in direct contact with the underlying electrode.

CV measurements indicate that the MOF is capable of electrocatalysis, exhibiting in CO_2-saturated solutions a catalytic wave at and before that for the catalytically active Fe(I/0) redox couple. CPE at a CO_2/CO overpotential of ∼650 mV yielded current densities of a few to several milliamperes per square centimeter, corresponding to the formation of CO and H_2, in roughly equal amounts, with a Faradaic efficiency of ∼100%. These products constitute a potential feedstock for Fischer−Tropsch synthesis of hydrocarbons. The observed catalytic currents are limited by the rate of diffusion of charge through the MOF, rather than by the molecular-scale kinetics of reaction of CO_2 with Fe-TPP. Enhancing the rate of diffusion clearly will be necessary for fully realizing the promise of Fe_MOF-525 or related materials as electrocatalysts; this is a focus of current work. In the presence of 1 M TFE as a weakly acidic proton donor, electrocatalysis persists for ∼5 h (albeit, with gradual decay, because of catalyst chemical degradation[7,72]).

We believe that our work represents a significant step forward in the heterogenization of molecular electrocatalysts for energy-relevant reactions under high-flux conditions. We are currently evaluating the broader utility of this approach to electrocatalysis, with an eye toward applications relevant to solar energy conversion.

ASSOCIATED CONTENT

Supporting Information

The Supporting Information is available free of charge on the ACS Publications website at DOI: 10.1021/acscatal.5b01767.

Experimental details, SEM, EDS, spectroelectrochemistry, and homogeneous Fe-TPP CPE (PDF)

AUTHOR INFORMATION

Corresponding Authors

*E-mail: j-hupp@northwestern.edu.
*E-mail: o-farha@northwestern.edu.
*E-mail: ckubiak@ucsd.edu.

Notes

The authors declare no competing financial interest.

DOI: 10.1021/acscatal.5b01767
ACS Catal. 2015, 5, 6302−6309

■ ACKNOWLEDGMENTS

The work at Northwestern University was supported as part of the ANSER Center, an Energy Frontier Research Center funded by the U.S. Department of Energy, Office of Science, Office of Basic Energy Sciences, via Award DE-SC0001059. I.H. thanks the U.S.–Israel Fulbright program for a postdoctoral fellowship. C.P.K. acknowledges support from a grant from the Air Force Office of Scientific Research, MURI Program (Award FA9550-10-1-0572).

■ REFERENCES

(1) Smieja, J. M.; Benson, E. E.; Kumar, B.; Grice, K. A.; Seu, C. S.; Miller, A. J. M.; Mayer, J. M.; Kubiak, C. P. *Proc. Natl. Acad. Sci. U. S. A.* **2012**, *109*, 15646−15650.
(2) Benson, E. E.; Kubiak, C. P.; Sathrum, A. J.; Smieja, J. M. *Chem. Soc. Rev.* **2009**, *38*, 89−99.
(3) Kumar, B.; Llorente, M.; Froehlich, J.; Dang, T.; Sathrum, A.; Kubiak, C. P. *Annu. Rev. Phys. Chem.* **2012**, *63*, 541−569.
(4) Saveant, J. M. *Chem. Rev.* **2008**, *108*, 2348−2378.
(5) Bonin, J.; Robert, M.; Routier, M. *J. Am. Chem. Soc.* **2014**, *136*, 16768−16771.
(6) Costentin, C.; Drouet, S.; Robert, M.; Saveant, J. M. *Science* **2012**, *338*, 90−94.
(7) Hammouche, M.; Lexa, D.; Momenteau, M.; Saveant, J. M. *J. Am. Chem. Soc.* **1991**, *113*, 8455−8466.
(8) Bhugun, I.; Lexa, D.; Saveant, J. M. *J. Am. Chem. Soc.* **1994**, *116*, 5015−5016.
(9) Bhugun, I.; Lexa, D.; Saveant, J. M. *J. Phys. Chem.* **1996**, *100*, 19981−19985.
(10) Costentin, C.; Passard, G.; Robert, M.; Saveant, J. M. *J. Am. Chem. Soc.* **2014**, *136*, 11821−11829.
(11) Agarwal, J.; Fujita, E.; Schaefer, H. F.; Muckerman, J. T. *J. Am. Chem. Soc.* **2012**, *134*, 5180−5186.
(12) Hawecker, J.; Lehn, J. M.; Ziessel, R. *J. Chem. Soc., Chem. Commun.* **1983**, *9*, 536−538.
(13) Sampson, M. D.; Froehlich, J. D.; Smieja, J. M.; Benson, E. E.; Sharp, I. D.; Kubiak, C. P. *Energy Environ. Sci.* **2013**, *6*, 3748−3755.
(14) Benson, E. E.; Sampson, M. D.; Grice, K. A.; Smieja, J. M.; Froehlich, J. D.; Friebel, D.; Keith, J. A.; Carter, E. A.; Nilsson, A.; Kubiak, C. P. *Angew. Chem., Int. Ed.* **2013**, *52*, 4841−4844.
(15) Chabolla, S. A.; Dellamary, E. A.; Machan, C. W.; Tezcan, F. A.; Kubiak, C. P. *Inorg. Chim. Acta* **2014**, *422*, 109−113.
(16) Song, J. S.; Klein, E. L.; Neese, F.; Ye, S. F. *Inorg. Chem.* **2014**, *53*, 7500−7507.
(17) Froehlich, J. D.; Kubiak, C. P. *Inorg. Chem.* **2012**, *51*, 3932−3934.
(18) Thoi, V. S.; Kornienko, N.; Margarit, C. G.; Yang, P. D.; Chang, C. J. *J. Am. Chem. Soc.* **2013**, *135*, 14413−14424.
(19) Schneider, J.; Jia, H. F.; Kobiro, K.; Cabelli, D. E.; Muckerman, J. T.; Fujita, E. *Energy Environ. Sci.* **2012**, *5*, 9502−9510.
(20) Jeletic, M. S.; Mock, M. T.; Appel, A. M.; Linehan, J. C. *J. Am. Chem. Soc.* **2013**, *135*, 11533−11536.
(21) Lacy, D. C.; McCrory, C. C. L.; Peters, J. C. *Inorg. Chem.* **2014**, *53*, 4980−4988.
(22) Bourrez, M.; Molton, F.; Chardon-Noblat, S.; Deronzier, A. *Angew. Chem., Int. Ed.* **2011**, *50*, 9903−9906.
(23) Sampson, M. D.; Nguyen, A. D.; Grice, K. A.; Moore, C. E.; Rheingold, A. L.; Kubiak, C. P. *J. Am. Chem. Soc.* **2014**, *136*, 5460−5471.
(24) Grills, D. C.; Farrington, J. A.; Layne, B. H.; Lymar, S. V.; Mello, B. A.; Preses, J. M.; Wishart, J. F. *J. Am. Chem. Soc.* **2014**, *136*, 5563−5566.
(25) Chen, Z. F.; Concepcion, J. J.; Brennaman, M. K.; Kang, P.; Norris, M. R.; Hoertz, P. G.; Meyer, T. J. *Proc. Natl. Acad. Sci. U. S. A.* **2012**, *109*, 15606−15611.
(26) Tamaki, Y.; Morimoto, T.; Koike, K.; Ishitani, O. *Proc. Natl. Acad. Sci. U. S. A.* **2012**, *109*, 15673−15678.
(27) Chen, Z. F.; Concepcion, J. J.; Jurss, J. W.; Meyer, T. J. *J. Am. Chem. Soc.* **2009**, *131*, 15580−15581.
(28) Lieber, C. M.; Lewis, N. S. *J. Am. Chem. Soc.* **1984**, *106*, 5033−5034.
(29) Yoshida, T.; Tsutsumida, K.; Teratani, S.; Yasufuku, K.; Kaneko, M. *J. Chem. Soc., Chem. Commun.* **1993**, *7*, 631−633.
(30) Parkin, A.; Seravalli, J.; Vincent, K. A.; Ragsdale, S. W.; Armstrong, F. A. *J. Am. Chem. Soc.* **2007**, *129*, 10328−10329.
(31) Yao, S. A.; Ruther, R. E.; Zhang, L. H.; Franking, R. A.; Hamers, R. J.; Berry, J. F. *J. Am. Chem. Soc.* **2012**, *134*, 15632−15635.
(32) Kang, P.; Zhang, S.; Meyer, T. J.; Brookhart, M. *Angew. Chem., Int. Ed.* **2014**, *53*, 8709−8713.
(33) Blakemore, J. D.; Gupta, A.; Warren, J. J.; Brunschwig, B. S.; Gray, H. B. *J. Am. Chem. Soc.* **2013**, *135*, 18288−18291.
(34) O'Toole, T. R.; Sullivan, B. P.; Bruce, M. R. M.; Margerum, L. D.; Murray, R. W.; Meyer, T. J. *J. Electroanal. Chem. Interfacial Electrochem.* **1989**, *259*, 217−239.
(35) Cabrera, C. R.; Abruna, H. D. *J. Electroanal. Chem. Interfacial Electrochem.* **1986**, *209*, 101−107.
(36) O'Toole, T. R.; Margerum, L. D.; Westmoreland, T. D.; Vining, W. J.; Murray, R. W.; Meyer, T. J. *J. Chem. Soc., Chem. Commun.* **1985**, *20*, 1416−1417.
(37) Collombdunandsauthier, M. N.; Deronzier, A.; Ziessel, R. *Inorg. Chem.* **1994**, *33*, 2961−2967.
(38) Portenkirchner, E.; Gasiorowski, J.; Oppelt, K.; Schlager, S.; Schwarzinger, C.; Neugebauer, H.; Knor, G.; Sariciftci, N. S. *ChemCatChem* **2013**, *5*, 1790−1796.
(39) Ramos Sende, J. A. R.; Arana, C. R.; Hernandez, L.; Potts, K. T.; Keshevarzk, M.; Abruna, H. D. *Inorg. Chem.* **1995**, *34*, 3339−3348.
(40) Morris, W.; Volosskiy, B.; Demir, S.; Gandara, F.; McGrier, P. L.; Furukawa, H.; Cascio, D.; Stoddart, J. F.; Yaghi, O. M. *Inorg. Chem.* **2012**, *51*, 6443−6445.
(41) Sathrum, A. J.; Kubiak, C. P. *J. Phys. Chem. Lett.* **2011**, *2*, 2372−2379.
(42) Note that once a monolayer of molecular catalyst has been immobilized, further catalyst immobilization increases the areal concentration (two-dimensional concentration), but not the volumetric (i.e., molar) concentration.
(43) Betard, A.; Fischer, R. A. *Chem. Rev.* **2012**, *112*, 1055−1083.
(44) We note that MOFs have been utilized before for photocatalytic CO_2 reduction;[45−47] however, as far as we know, there is no report of electrochemical CO_2 reduction with molecular catalyst-based MOFs.
(45) Wang, C.; Xie, Z. G.; deKrafft, K. E.; Lin, W. L. *J. Am. Chem. Soc.* **2011**, *133*, 13445−13454.
(46) Wang, D. K.; Huang, R. K.; Liu, W. J.; Sun, D. R.; Li, Z. H. *ACS Catal.* **2014**, *4*, 4254−4260.
(47) Zhang, T.; Lin, W. B. *Chem. Soc. Rev.* **2014**, *43*, 5982−5993.
(48) Ahrenholtz, S. R.; Epley, C. C.; Morris, A. J. *J. Am. Chem. Soc.* **2014**, *136*, 2464−2472.
(49) Hod, I.; Bury, W.; Karlin, D. M.; Deria, P.; Kung, C.-W.; Katz, M. J.; So, M.; Klahr, B.; Jin, D.; Chung, Y.-W.; Odom, T. W.; Farha, O. K.; Hupp, J. T. *Adv. Mater.* **2014**, *26*, 6295−6300.
(50) Wade, C. R.; Li, M. Y.; Dinca, M. *Angew. Chem., Int. Ed.* **2013**, *52*, 13377−13381.
(51) Usov, P. M.; Fabian, C.; D'Alessandro, D. M. *Chem. Commun.* **2012**, *48*, 3945−3947.
(52) Hod, I.; Bury, W.; Gardner, D. M.; Deria, P.; Roznyatovskiy, V.; Wasielewski, M. R.; Farha, O. K.; Hupp, J. T. *J. Phys. Chem. Lett.* **2015**, *6*, 586−591.
(53) Kosal, M. E.; Chou, J. H.; Wilson, S. R.; Suslick, K. S. *Nat. Mater.* **2002**, *1*, 118−121.
(54) Furuya, N.; Matsui, K. *J. Electroanal. Chem. Interfacial Electrochem.* **1989**, *271*, 181−191.
(55) Kung, C.-W.; Chang, T.-H.; Chou, L.-Y.; Hupp, J. T.; Farha, O. K.; Ho, K.-C. *Chem. Commun.* **2015**, *51*, 2414−2417.
(56) Mondloch, J. E.; Katz, M. J.; Planas, N.; Semrouni, D.; Gagliardi, L.; Hupp, J. T.; Farha, O. K. *Chem. Commun.* **2014**, *50*, 8944−8946.
(57) DeCoste, J. B.; Peterson, G. W.; Jasuja, H.; Glover, T. G.; Huang, Y. G.; Walton, K. S. *J. Mater. Chem. A* **2013**, *1*, 5642−5650.

DOI: 10.1021/acscatal.5b01767
ACS Catal. 2015, 5, 6302−6309

(58) Gomes Silva, C. G.; Luz, I.; Llabrés i Xamena, F. X.; Corma, A.; Garcia, H. *Chem.—Eur. J.* **2010**, *16*, 11133−11138.
(59) Vermoortele, F.; Ameloot, R.; Vimont, A.; Serre, C.; De Vos, D. *Chem. Commun.* **2011**, *47*, 1521−1523.
(60) Hwang, Y.; Sohn, H.; Phan, A.; Yaghi, O. M.; Candler, R. N. *Nano Lett.* **2013**, *13*, 5271−5276.
(61) Cardona, C. M.; Li, W.; Kaifer, A. E.; Stockdale, D.; Bazan, G. C. *Adv. Mater.* **2011**, *23*, 2367−2371.
(62) Because NHE is, strictly speaking, ill-defined in acid-free acetonitrile, we note that the potential of ferrocene(+/0) versus NHE in acetonitrile is 0.597 V. In practice, the solvent contains residual water. Note that even 0.1% residual water by volume is still more than 50 mM water.
(63) The TOF that corresponds to the CPE peak current density is 5.6 h^{-1}.
(64) Georgopoulos, M.; Hoffman, M. Z. *J. Phys. Chem.* **1991**, *95*, 7717−7721.
(65) Dry, M. E. *Catal. Today* **2002**, *71*, 227−241.
(66) Bhugun, I.; Lexa, D.; Saveant, J. M. *J. Am. Chem. Soc.* **1996**, *118*, 1769−1776.
(67) Costentin, C.; Drouet, S.; Passard, G.; Robert, M.; Saveant, J. M. *J. Am. Chem. Soc.* **2013**, *135*, 9023−9031.
(68) TFE addition also serves to better define the proton activity of the reaction solution. In turn, this allows us to estimate the thermodynamic potential (formal potential, Ef) for the reaction CO_2 + 2H + 2e^- → CO + H_2O. Following Saveant, and recognizing that TFE is a weaker acid than water, we find the estimated values are −0.650 and −0.694 V versus NHE for acetonitrile and DMF, respectively. Thus, catalysis measurements at E = −1.3 V versus NHE correspond to a kinetic overpotential of approximately 0.60−0.65 V. For integrated photoelectrochemical cells designed to convert CO_2 to CO as a solar fuel, it has been suggested that overpotentials of up to 700 mV could be tolerated under conditions where the photocurrent density, without light concentration, is 10 mA/cm^2. An integrated cell, of course, would likely need to operate in water as solvent, to accommodate oxidation of water to O_2 as the complementary half-reaction. To facilitate comparisons with the sizable literature on FeTPP and related spcies as molecular electrocatalysts, we have intentionally employed nominally nonaqueous solvents.
(69) A reviewer has suggested that acidic protons on the MOF node, although located ∼10 Å from the iron site (active site), might function as cocatalysts for H_2 formation, thereby accounting for the greater importance of H_2 formation with the MOF-based catalyst relative to the homogeneous version of the catalyst.
(70) Costentin, C.; Drouet, S.; Robert, M.; Saveant, J. M. *J. Am. Chem. Soc.* **2012**, *134*, 11235−11242.
(71) We note that there are other possible factors that could influence the catalytic activity of the MOF. During catalysis, the pH increases as CO_2 is reduced because of the loss of protons to produce the water as a coproduct. Some of the base will combine with CO_2 to decrease its effective concentration. Thus, ingress/egress of reagents and products through the porous film is clearly a factor that will affect the overall TOF of the MOF.
(72) The MOF-525 film remains following electrolysis for 5 h but is less intensely colored than before electrolysis. We speculate that chemical reduction of the porphyrin (and loss of aromaticity) eventually occurs but have not investigated further. The catalytic activity of the homoegenous catalyst is also known to decay over the course of hours if no proton source is added to solution.

DOI: 10.1021/acscatal.5b01767
ACS Catal. 2015, 5, 6302−6309